Measurement of Unsteady Aerodynamic Data in Turbomachinery Periodic Flows

Jan Lepicovsky*, and *David* Šimurda

Institute of Thermomechanics of the Czech Academy of Sciences, Dolejskova 1402/5, 182 00, Prague, Czech Republic

Abstract. The objective of this work is to demonstrate the feasibility and advantage of an alternative approach to aerodynamic data acquisition in high-speed highly-loaded turbine engine rotating components. Two methodologies of data acquisition using fast sensing pressure probes are described here. The conventional approach is based on using separate probes for detection of unsteady total and static pressures and the flow direction. This method is labor intensive, requiring either multiple access ports on the investigated engine or repetitive test runs for each individual probe if only one access port is available. An alternative method, using only one Pitot-cylinder probe, can be used to acquire total pressure and flow direction data. The Pitot-cylinder probe basically functions like a controlled flow direction follower. The data reduction procedure for this probe relies on strict periodicity of the investigated flow during a test run. A detailed explanation of data reduction procedure and examples of achieved results are presented.

1 Introduction

Advances in turbine engine technology have always been dependent on a better understanding of complex flow phenomena in the engine flow paths involved in energy transfer. The main unsteady aerodynamic parameters which are of interest to turbine engine designers, are local pressures and flow velocity vectors. Several experimental methodologies, allowing for the detection of rapidly changing flow parameters, evolved over the years, which include miniature high frequency pressure transducers, thermo-anemometry, and nonintrusive optical methods. For practical reasons only fast-sensing pressure probes can be effectively used for industrial research on real turbine engines.

An excellent overview of the unsteady probe technology status and probe utilization for turbomachinery research in leading laboratories has been given in Refs. 1 through 5. The authors of this paper apologize to those whose important contributions are not reported here. It is just an unfortunate oversight, not an intentional omission. Focus of this paper is solely on developments carried out at NASA GRC in the past decade.

2 Ideal probe for turbomachinery unsteady flow research

An ideal aerodynamic probe for unsteady data measurements should satisfy three main criteria:

High frequency response
The ideal probe must be able to follow the rapid changes of flow parameters.

Simultaneous detection
The ideal probe with multiple sensors should detect flow parameters at the same time.

High spatial (angular) resolution
The ideal probe should detect flow parameters at a single point in space.

It will later be pointed out that only two of these criteria can be satisfied at the same time for real probes.

Optical techniques are not very practical in turbine engine research. Thermo-anemometry is an excellent method for low velocity high turbulence flow research. However, thermo-anemometric probes are not suitable for high speed turbomachinery applications due to the decreasing probe sensitivity with increasing flow velocity, and to high probe fragility. It follows that the fast response pressure probes are still the only reliable and practical methodology for internal unsteady flow measurements in real turbine engines. The pros and cons of these experimental techniques are summarized in the following tables (Tab. 1 and Tab. 2.)

3 Selection of data acquisition methodology

The ultimate goal of the research effort reported here was to develop a reliable and affordable methodology for aerodynamic unsteady data acquisition in high speed and highly loaded rotating full scale components of real turbomachines. The focus was on acquiring distributions of total pressure and velocity direction of flow exiting from the rotating component exit plane. The goal was to limit the probe head size in order to

* Corresponding author: lepic@it.cas.cz

Table 1. Basic features of thermos-anemometric probes

UNSTEADY PRESSURE PROBES Total pressure, static pressure, wedge probes
▲ High frequency response. ▼ Lower spatial resolution and larger size. ▲ Increasing sensitivity with increasing flow velocity. ▲ Maximum allowable flow temperature up to 550 K (277 C). ▲ Very good sensor protection
Suitable for highly-loaded, high-speed turbomachines.

Table 2. Properties of fast response pressure probes

THERMO-ANEMOMETRIC PROBES Single hot-wire, cross hot-wire, split-fiber probes
▲ High frequency response. ▲ Superior spatial resolution in cross flow. ▼ Rapidly decreasing sensitivity with increasing flow velocity. ▼ Maximum allowable flow temperature up to 390 K (117 C). ▼ Very high probe fragility.
Suitable for lightly-loaded, low-speed turbomachines.

prevent any side effects of flow blockage due to probe insertions. Based on this requirement, it was concluded that no probe with more than two built-in miniature pressure transducers will be considered.

Two approaches were contemplated. The first one, called TP-WP (total pressure and wedge probes), relies on two separate probes, one for flow direction measurement and the other for the total pressure measurement. The second approach, called PC (Pitot cylinder), is based on a single probe that is used as a flow direction follower that, when properly oriented, would record also the flow total pressure. Both approaches have some advantages and also some drawbacks.

A WP determines the flow direction by sensing pressure levels on sides of the probe wedge. It can be used in periodic, random or transient flows, and the probe will detect data in both probe pressure taps simultaneously.

However, there is a caveat here: in the TP-WP setup, the probes will be always some distance apart, so in no case it is a single point of measurement in a given flowfield. This is a significant drawback of this approach. A measurement at the exit plane of a compressor or turbine rotor can be made in two ways. First, having only a single access probe port on a rotor shell, two subsequent test runs must be made with swapped probes, which is labor intensive and violates the simultaneity of data acquisition. Furthermore, the accuracy of the test results strongly depends on setting the identical operation conditions for both runs. If two access ports are available, then data can be acquired concurrently although at very separate locations, and the question arises how representative these data are for a single point measurement.

In the second approach, called PC, only one probe is used and the flow direction and total pressure are detected at the very same location in the investigated flowfield. The dilemma here is that while measuring at a single point, the probe must be actively rotated to several different yaw angle orientations in order to detect the true flow direction, which requires a prolonged test run while keeping the steady operation conditions at all time. Details of this methodology will be explained later. The major drawback is that it can be applied only to strictly periodic flows, which luckily most of the operation condition turbomachinery flows are. From an overall point of view, the PC approach is cost effective. Only one probe with a miniature pressure transducer is needed and only one probe port in the machine shell is required. The PC test runs are albeit longer; nonetheless no test interruption and necessary and involved probe swapping is needed as is the case with the TP-WP approach.

A decision was made in favor of using the PC approach for upcoming research measurements in a highly-loaded high-speed radial impeller. However, it was also suggested to first verify the PC methodology by making comparative measurements with the TP-WP approach in a low-speed research axial compressor to further substantiate the decision in favor of the PC methodology.

4 Wedge probe design, assembly and calibration

The unsteady total pressure probe, labeled TP, was already available from a previous research task [Ref. 6]. Its design is relatively simple. It was based on a design reported in Ref. 7. A schematic and photographs of individual components of the total pressure probe are in Fig. 1. A modified miniature pressure transducer was inserted in the probe stem with its diaphragm facing the end of a very short inlet receiving duct. The probe had overall natural frequency of 30 kHz.

The wedge probe design, shown in Fig. 2, was much more demanding. It is necessary to accommodate two pressure transducers in the probe head and keep the sensing taps as close to each other as possible. As seen in Fig. 2, the ducts were laid out to be of the same length. Cutaway drawings of the left and right pressure taps are in the same figure. The radiogram in lower half of Fig. 3 depicts the inner layout of the completed probe. It is believed this is the smallest arrangement for a wedge probe head design at present using available and affordable commercial miniature pressure

transducers. The resulting overall natural frequency of the wedge is 20 kHz.

Miniature pressure transducers, model Kulite XCS-062-15D with modified extended length, were used in the probes designed at NASA GRC. The transducers in the TP and PC probes were easily sealed applying a drop of adhesive at the head end. However, the wedge probe has deep sockets for both transducers inside the wedge probe head, and they are not easily accessible. The transducer sockets must be sealed to avoid possible crosstalk between the pressure taps, which would denigrate the wedge probe directional accuracy. Therefore, both transducers were first bonded into a clamp as shown in Fig. 4. Then both transducers were lightly coated with a band of an adhesive about 10 mm away from their tips, and the transducer subassembly was then gently pushed inside the probe head. A view of the pressure transducer duo before insertion in the wedge probe stem and head is in Fig. 5.

Completed wedge probe was subjected to rigorous calibrations, both static (for the pressure transducers) and steady flow (probe head) characteristics. Steady flow calibration was performed in a free jet exiting in ambient air for the velocity dependence as well as for the directional characteristic. Typical results for the wedge probe yaw angle calibration are shown in Fig. 6 in terms of yaw angle direction coefficient (Eq. 1).

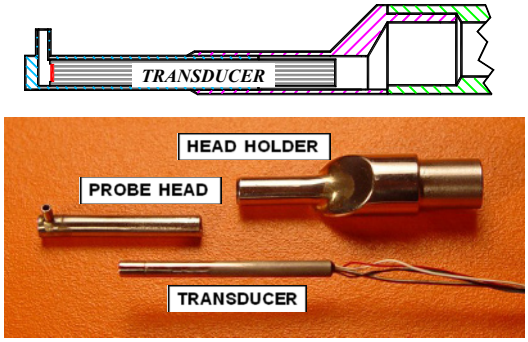

Fig. 1. Fast-response total pressure probe (NASA GRC)

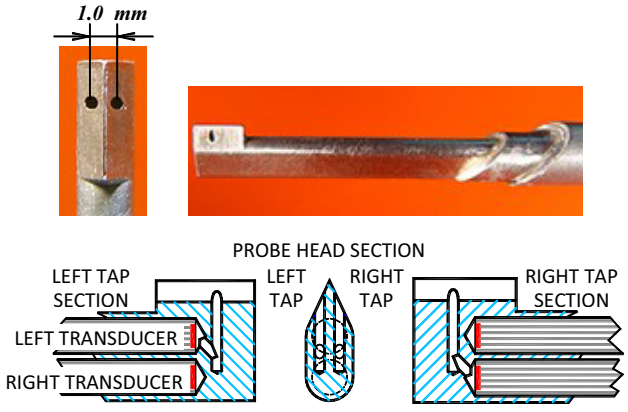

Fig. 2. Wedge flow direction probe (NASA GRC)

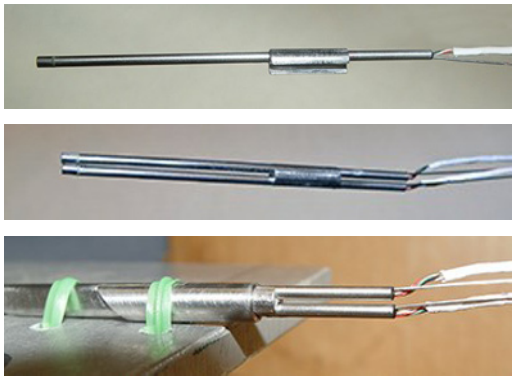

Fig. 4. Stages in wedge probe assembly

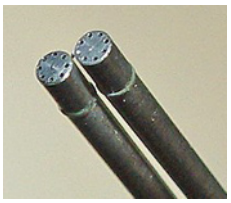

Fig. 5. Two transducers Kulite XCS-062x with protective screens

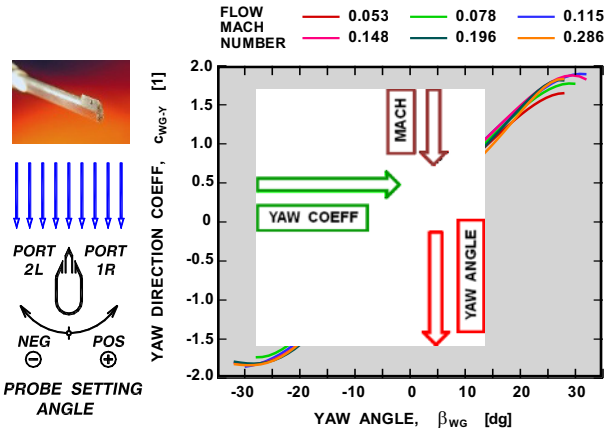

Fig. 6. Velocity and flow direction calibration characteristic of wedge probe (NASA GRC)

$$c_{WG-Y} = \frac{p_{1R} - p_{2L}}{p_T - p_S} \quad (1)$$

c_{WG-Y}	[1]	WP yaw angle coefficient
p_{1R}	[kPa]	probe right tap pressure
p_{2L}	[kPa]	probe left tap pressure
p_T	[kPa]	total (plenum) pressure
p_S	[kPa]	static (ambient) tap pressure

5 Pitot-cylinder probe design and application methodology

The Pitot-cylinder probe is shown in Fig. 7. Its design is nearly identical to the total pressure probe shown in Fig. 1. The only difference is the absence of the short inlet receiving duct, which is replaced with a simple pressure tap on the cylinder surface. This design modification increases the PC probe overall natural frequency to 65 kHz. A directional yaw angle calibration characteristic of the Pitot-cylinder probe is given in Fig. 8, and the yaw angle coefficient is in Eq. 2.

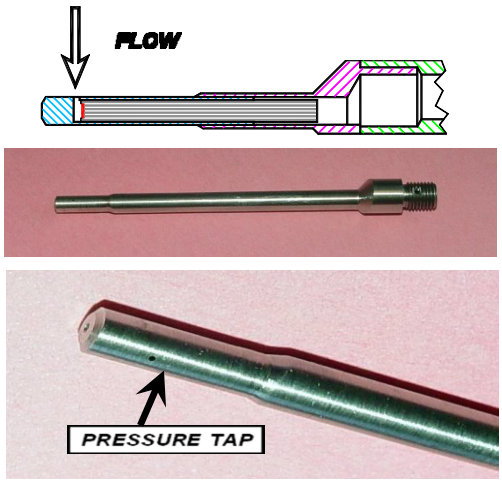

Fig. 7. Fast response Pitot-cylinder pressure probe (NASA GRC)

$$c_{PC-Y} = \frac{p_M - p_S}{p_T - p_S} \quad (2)$$

c_{PC-Y}	[1]	PC yaw angle coefficient
p_M	[kPa]	detected pressure level
p_T	[kPa]	total (plenum) pressure
p_S	[kPa]	static (ambient) tap pressure

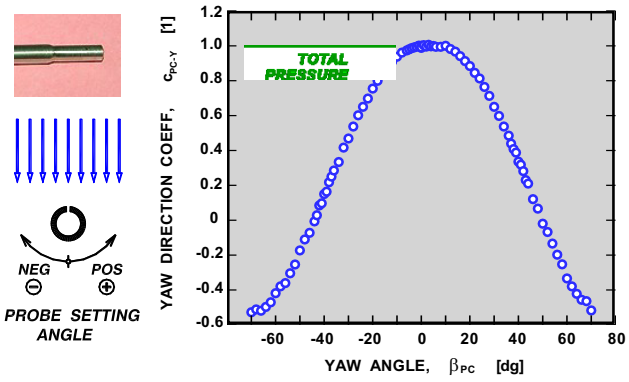

Fig. 8. Yaw direction coefficient of Pitot-cylinder pressure probe (NASA GRC)

The Pitot-cylinder probe is a very small, single transducer device capable of multi-parameter measurement, albeit only in the time-repetitive periodic flow mode. It was revealed later that a probe of a similar design was reported in Ref. 5. However, the results reported here were obtained independently, and the task was conceived without any prior knowledge of the effort reported in Ref. 5.

In theory, the Pitot-cylinder probe can be used for total pressure, inflow static pressure, and flow angle measurements. As will be indicated further, in practice only the total pressure and flow direction can be measured reliably. The probe satisfies two of the three ideal probe criteria, namely the high frequency response and a high spatial resolution. A drawback of this probe is that repetitive data acquisition must be performed to acquire the desired unsteady flow parameters. Consequently, the probe can be fully utilized only in strictly periodic flows. Flows in turbomachine rotating components satisfy this condition. In complex 3D transient flow situations, this probe can be used only with utmost caution.

The probe stem has a diameter of only 3 mm, and the pressure receiving port is 0.4 mm in diameter. The pressure receiving tap is positioned exactly on the axis of rotation of the probe holder. The probe must be progressively turned in yaw direction during the data gathering phases and it is important that the pressure receiving tap always stays fixed in the same point in the coordinate reference frame.

The data acquisition methodology for Pitot-cylinder probes is based on the knowledge of a surface pressure distribution pattern on a circular cylinder in transverse flows. The lack of directional characteristic symmetry in Fig. 8 should be noticed. An obvious reason for it is a poorer detection of local surface pressure values. It is caused by pressure partial averaging due to a relatively large size of the pressure-sensing orifice with respect to the probe diameter. The diameter of the pressure-sensing tap stretches over 15 dg of the cylinder circumference, although the orifice alone is actually only 0.4 mm wide. These two dimensions inherently contradict each other in an effort to miniaturize the probe size even further. Consequently, this probe cannot be used reliably for inflow static pressure measurements.

When any probe is inserted in a flow behind a spinning rotor, then the probe is exposed to a varying angle of flow incidence, which regularly repeats with each rotor blade passing by the probe. This situation is depicted in Fig. 9. In the case of the Pitot-cylinder probe, the varying flow pattern about the probe is identical to the one about a cylinder in steady crossflow, albeit with a periodically oscillating flow stagnation point on a segment of the probe circumference as shown here. Situations for two probe yaw setting angles are depicted here, the one for ωPC = -35 dg is shown by the upper group and the situation for other probe setting angle of ωPC = -55 dg is shown by the lower group of sketches. The setting angle values are of a rotor absolute coordinate frame.

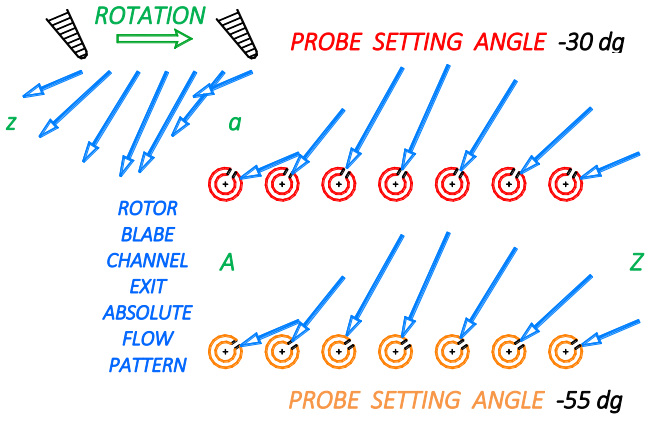

Fig. 9. Phase out velocity vectors for blade channel absolute flow phasing by Pitot-cylinder probe; two probe setting yaw angles are shown.

As seen here, the velocity vector, or flow stagnation point, regularly crosses the probe pressure tap at the same instances of the blade channel flyby period. Of course, the exact timing when the velocity vector

crosses the pressure tap depends on the probe setting angle, provided all other operation parameters do not change. It is obvious if one compares the series of sketches in the upper and lower sets in Fig. 9. Evidently, when the velocity vector crosses the pressure tap and points in the center of the probe cylinder, it is the instant when the immediate flow total pressure is sensed. At the same instant the probe setting angle also coincides with the velocity angle immediate direction. It should be noted that the time sequence in the machine is from right to left (z ← a), whereas in the phased out probe sketches the time sequence is from left to right (A → Z).

Records of pressure transducer signals for six different probe yaw setting angles are shown in Fig. 10; any larger number of probe angle settings can be chosen in order to improve the measurement resolution. The green traces shown here are ensemble averages computed from many (usually several thousands) rotor blade passes continuously recorded. For clarity, two identical ensemble averages are plotted next to each other, thus the plotted data stretch over two blade passages. It must be emphasized here that the green traces are not the flow total pressure values. They are merely the probe cylinder surface pressures recorded at the probe particular yaw angle setting.

In the next step, separate sets of data will be created for chosen time instances within the time period of a blade channel bypassing the pressure probe. For example, two instances of τ_{BLP} = 0.2 and τ_{BLP} = 0.6 were selected, and data points to be collected are shown by small circles in Fig. 10. A plot resulting for the selected time instant e.g. of τ_{BLP} = 0.2 is shown in Fig. 11 (the first plot on the left hand side). As indicated in Fig. 9, there is always an instant when the velocity vector points directly in radial direction in the pressure sensing tap; obviously at this instant the tap is exposed to the immediate flow total pressure. The task is finding the peak value of the left plot in Fig. 11. In this case it is done by folding the data (middle plot) until the perfect match is found (right plot in Fig. 11). It follows that the coordinates of the plot peak in Fig. 11 represent the total pressure and the flow angle at this particular moment in time (τ_{BLP} = 0.2 in this selected case).

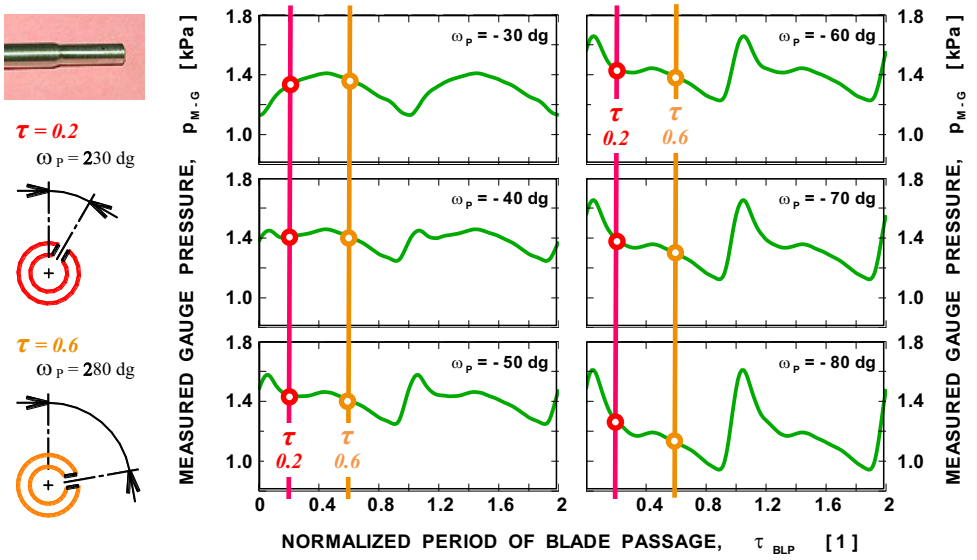

Fig. 10. Phase out blade channel flow passing by the Pitot-cylinder probe

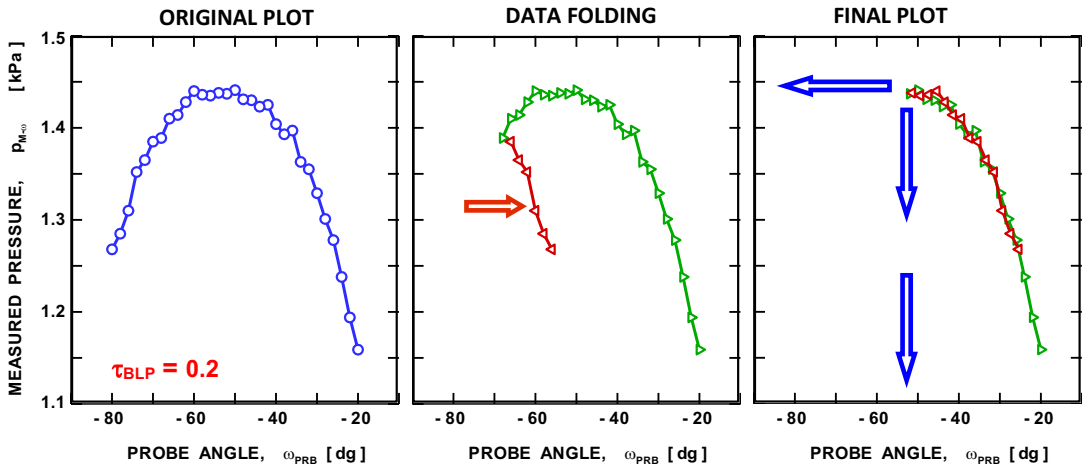

Fig. 11. Graphic interpretation of computer algorithm for finding flow angle and total pressure values

The process of building the final required distributions of flow parameters is indicated in Fig. 12; only the plot for the flow angle distribution is shown here for simplicity. Data points are plotted in sequence of selected and reduced pitch period station instances (τ_{BLP}). For example, if the first selected station is for τ_{BLP} = 0.2; this data point is represented by the first (red) small circle in plot in Fig. 12. If the second selected pitch period instant is τ_{BLP} = 0.6, then the next (orange) circle is added to the same plot. Proceeding in this manner for all blade channel pitch positions, the full blade channel distribution for the flow direction can be built (a blue curve in Fig. 12). Although the procedure seems to be quite involved, the entire process is semi-automated and actually requires only few initial entries into a computerized application.

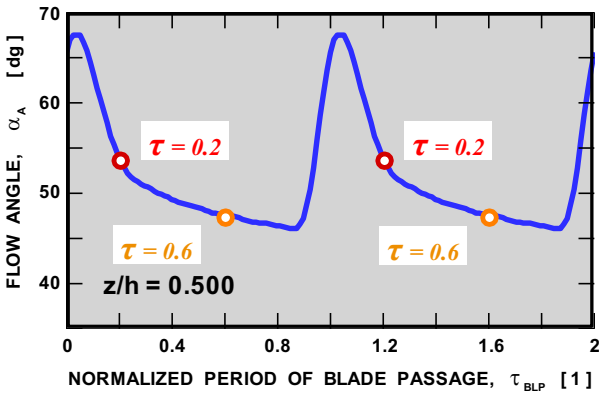

Fig. 12. Process of building absolute flow angle distribution along blade pitch

6 Testing in research low-speed axial compressor

The NASA GRC low-speed research axial compressor was selected for comparative testing of three aerodynamic probes: Pitot-cylinder probe, wedge directional probe and split-fiber thermo-anemometric probe. The reason was that the compressor flowfield was already well known based on previous extensive testing in this facility [Refs. 8 through 10].

To judge the probes' performance, only the flow direction data were compared because the first two probes can detect pressure and flow direction, whereas the split-fiber probe detects flow velocity and its direction. The compressor partial cross-section and the blade layout are shown in Fig. 13. Each rotor had 39 blades; each stator consisted of 52 vanes. The rotor blade pitch at mid-height was 89 mm, rotation speed was kept at 984 rpm, and thus the resulting blade passing frequency was 640 Hz only.

Velocity defects in the blade wake flow occur in the relative (rotating) frame of references, whereas the probes are located in the absolute frame. The wake flow is manifested in the absolute frame as variations in the flow direction rather than changes in the flow velocity as shown in velocity triangles depicted in Fig. 14.

The wedge probe performance can be judged on ability to detect the instantaneous variation in flow direction. Obviously, the probe performance will depend on spatial resolution of each of the probes. The probe heads, drawn in the same scale as the rotor blade trailing edge, are shown in Fig. 15. The split-fiber probe has a diameter of only 0.2 mm; it is pointed to by a red arrow in this figure. The distance between the centers of wedge probe taps is 1.0 mm (see Fig. 2). Actually the distance between the wedge probe tap outer edges is actually even greater, 1.4 mm.

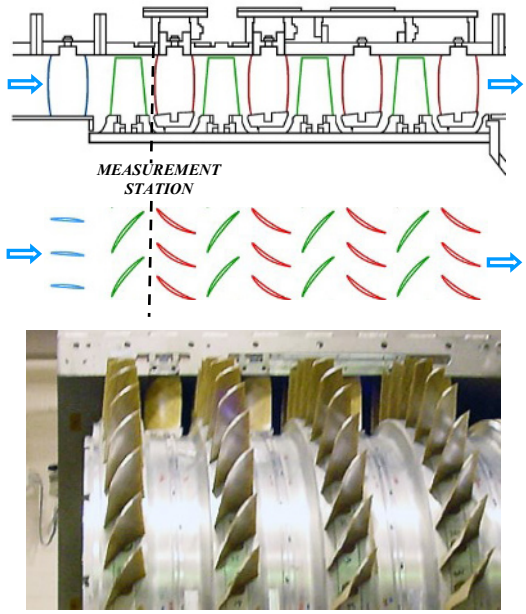

Fig. 13 Flow path and blading of the NASA low-speed axial compressor

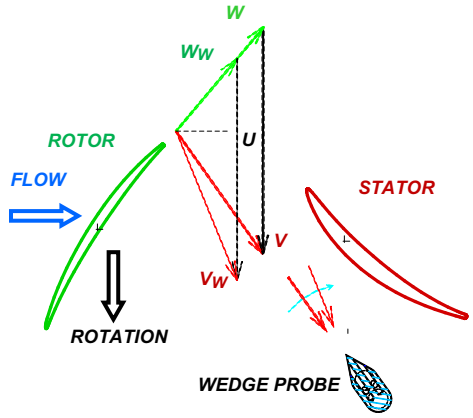

U	[m/s] circumferential velocity
V	[m/s] core flow absolute velocity
V_W	[m/s] wake region absolute velocity
W	[m/s] core flow relative velocity
W_W	[m/s] wake region relative velocity

Fig. 14. Compressor blading and velocity triangles

The results of the comparative test are shown in Fig. 16. Data acquired by all three probes are presented here. As indicated here, the split-fiber probe recorded maximum flow angle of 68 dg at the center of the blade wake, whereas the flow angle recorded by the wedge probe was only 62 dg. At the probe station, the width of the wake flow region was recorded as 20% and 27%

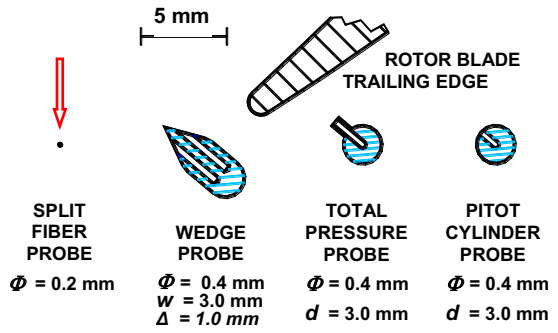

ϕ	[mm]sensing element dimension
d	[mm]probe head diameter (TP-PC)
w	[mm]probe head width (WP)
Δ	[mm]istance btw sensing ports (WP)

Fig. 15. Comparison of probe dimensions with rotor trailing edge

of the blade channel pitch by the split-fiber and wedge probes, respectively. Also, there is a small difference in timing of the wake region center. It appears that the wedge probe records the wake center with a small delay in comparison to the split-fiber probe. In terms of the blade pitch relative positions, the shift of the wedge probe trace is about 11% behind the split-fiber data.

The consequence of the distance between pressure taps on the probe wedge is that in regions of fast flow direction changes, each tap is "looking" at slightly different flow angles. The resulting probe signal represents an average of these two tap values. It follows that even such a miniature wedge probe as this one will not be able to detect sharp variations in the flow direction. The probe will thus smooth out (or filter) most of the fine details of the flow pattern under investigation as seen in Fig. 16 by lower peak flow angle value.

On the other hand, the agreement between the Pitot-cylinder probe data and split-fiber probe data is amazingly good. It proves three points. First, a pressure-sensing based probe can achieve nearly the same spatial resolution and measurement accuracy as a split-fiber thermo-anemometric probe for measure-ments in turbomachinery internal flows. Second, it validates the finding that the discrepancy between the split-fiber data and the wedge probe data was caused by insufficient spatial resolution of the later. And third, it confirms that the Pitot-cylinder probe can be reliably used for internal flow investi-gation in highly-loaded, high-speed turbomachines.

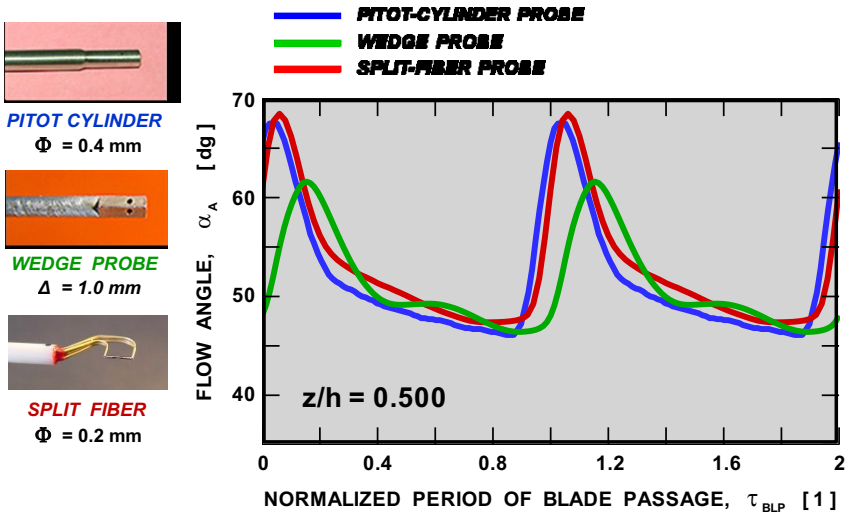

Fig. 16. Flow absolute angle distributions across rotor blade channel detected by Pitot-cylinder, wedge, and split-fiber probes

7 Investigation of exit flowfield of a high-speed radial impeller

A side view of a high-speed highly-loaded radial impeller to be tested is shown in Fig. 17. The impeller exit diameter is 431 mm, and the clear height of the exit channel is 17 mm. Impeller exit tip speed is 492 m.s-1, which is 21 789 rpm. The impeller has 15 main and 15 splitter blades. The blade passing frequency is 10.9 kHz (Ref. 11).

The testing in radial compressor proceeded in a similar manner as it was done in the low-speed axial compressor. The Pitot-cylinder probe was positioned in steps across the height of the impeller exit channel starting from the impeller back plate (x/H = 0). The probe receiving tap could not reach up to the impeller shroud; the last station was at x/H = 0.85. At each of the seven measurement stations, the probe was progressively oriented to ten yaw angles in increments of 10 dg starting in the range from -30 dg to 60 dg. The sets of unsteady pressure data were taken at each angle orientation. All together 70 data points were recorded, and each data set comprised of 50 000 samples. The sampling frequency was 50 kHz, which means that each acquisition period lasted for 363 rotor revolutions and/or 10 890 blade channel passes.

The acquired data sets were ensemble averaged over the length of the blade channel pitch. Samples of averaged data for two probe insertions of x/H = 0.85 and x/H = 0.06 are in Figs. 18 and 19, respectively. Seven groups of such data were recorded during the

channel height traversing. These plots are in a form similar to the plot shown already in Fig. 10. The subplots are arranged horizontally next to each other in order to better illustrate the changes in recorded pressure levels as the probe yaw angle changes. Data at each subplot is shown for two adjacent blade channels.

Each of the seven groups of data were sliced at selected time instants to generate the plots of instant pressure level dependence on the probe angle orientation. These plots were similar to the one in Fig. 11; however, each plot consisted of pressure levels for only 10 probe yaw angle settings. These data sets served in finding the probe angle for the maximum instant pressure at each blade pitch fraction.

It follows for the given sampling rate and the blade passing frequency that 92 samples were taken over a width of the blade channel, which is 45 mm wide. Therefore the data spatial resolution within the blade channel is 0,5 mm, which seems to be sufficient to register pressure and direction changes of sharp passing wakes.

Finally, having all data reduced and converted to instant total pressure levels and flow angles, the contour plots over an area of the rotor exit blade channel were created. The contours of exit total pressure and absolute flow angle are shown in Figs. 20 and 21, respectively. The total pressure contours are displayed in term of the pressure coefficient (Eq. 2)

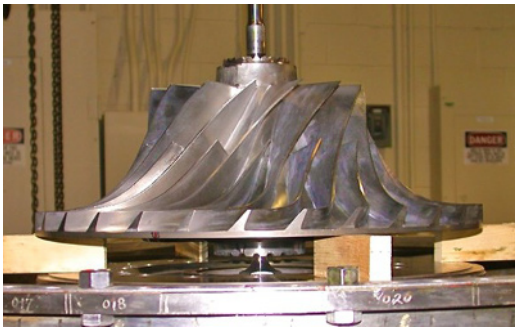

Fig. 17. View of the tested radial impeller

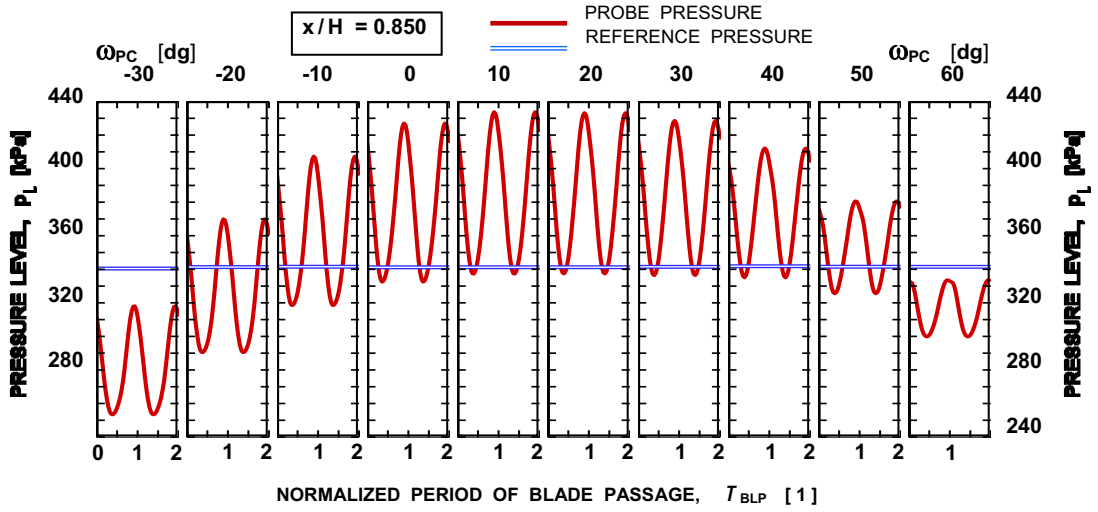

Fig. 18. Ensemble averages of PC probe pressure data for a set of yaw angle rientations taken at a station close to the impeller shroud

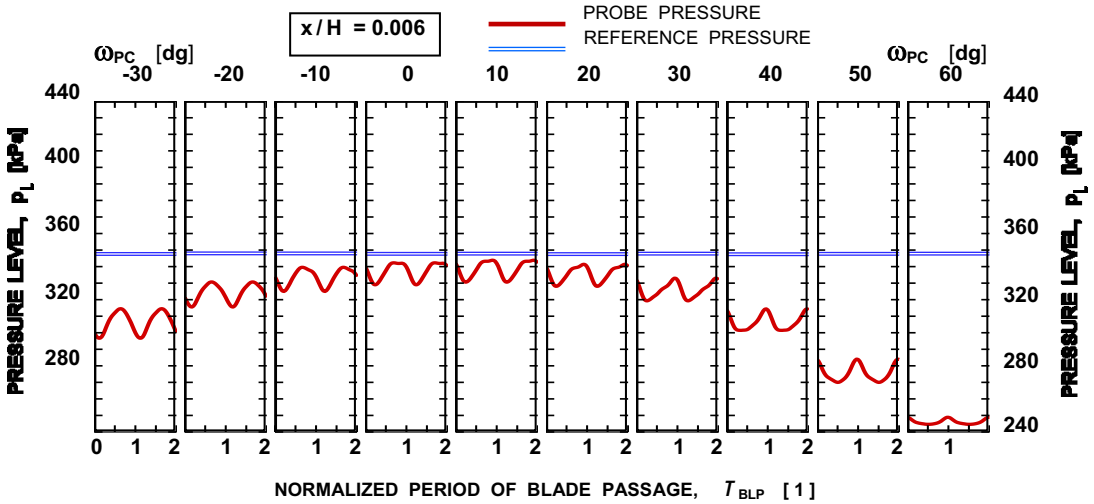

Fig. 19. Ensemble averages of PC probe pressure data for a set of yaw angle orientations taken at a station close to the impeller back plate

The contour pattern of the total pressure field at the impeller exit exhibits two distinct peaks close to the blade channel pressure side (PS) and a depression behind the tip of the blade channel suction surface (SS). It closely resembles the effects of the secondary flow pattern in an impeller channel reported in Ref. 12 (Fig. 22). Secondary flows transport the low energy fluid of the boundary layer along the blade surface. The area with the largest danger of separation is the shroud-suction side corner.

Both contour plots indicate the presence of the discharge flow structure shown in Fig. 23 (Ref. 13). The flow structure consists of low velocity zone or "wake" next to the suction surface, and necessarily, a "jet" flow of increased velocity in the rest of the blade channel. The jet-wake structure of the discharge flow is clearly indicated by total pressure distribution in Fig. 20. In the plot of absolute flow direction contour in Fig. 21, the jet portion of the flow is manifested by large absolute flow angle. The flow of the wake section has a small exit radial velocity in the relative (rotating) frame of the impeller. Therefore it is moving mostly in the tangential direction in the absolute frame of coordinates, which is indicated by the region of low absolute flow angle

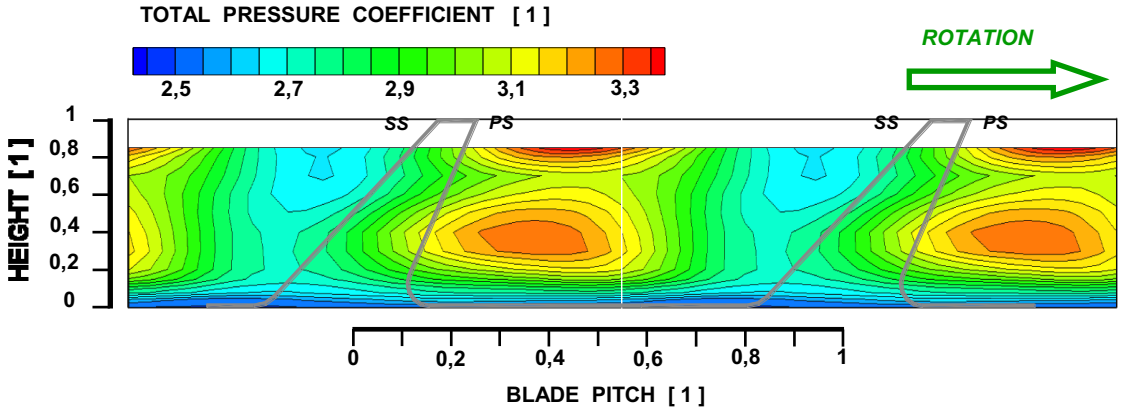

Fig. 20. Total pressure contours at the radial impeller exit blade channel

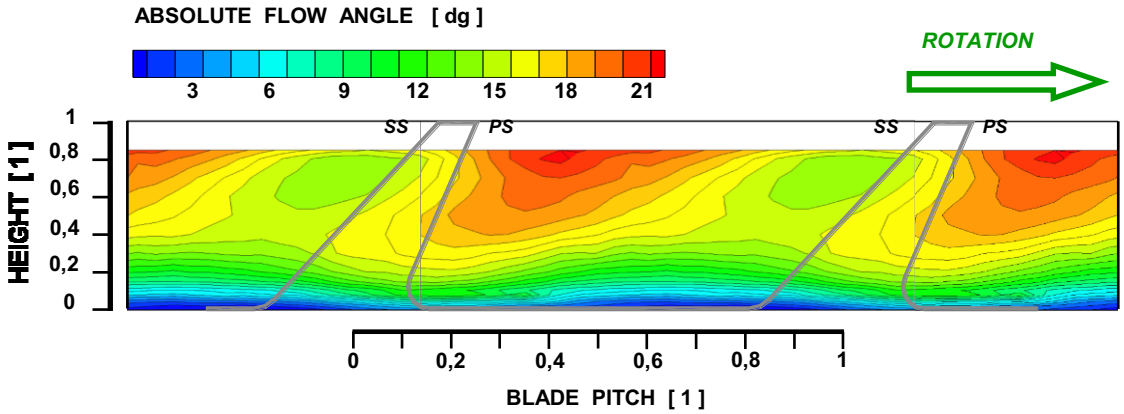

Fig. 21. Flow absolute angle contours at the radial impeller exit blade

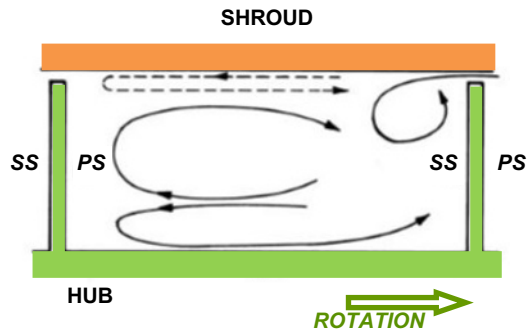

Fig. 22. Secondary flow pattern in a radial impeller exit channel

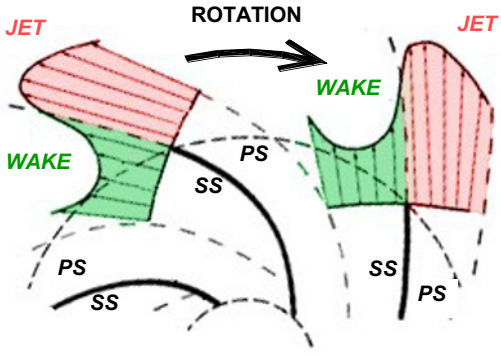

Fig. 23. Jet and wake structure of a radial impeller discharge flow

8 Conclusions

Based on the achieved experimental results, the following conclusions can be made.

First of all, the single transducer Pitot-cylinder probe and the devised data reduction methodology proved to be a viable alternative to multi-sensor probe approach for research investigation of unsteady periodic flows in turbomachines. The acquired discharge flow contours of highly-loaded, high-speed radial impeller clearly exhibit fine details reported elsewhere in the open technical literature.

Further, the angular resolution of the Pitot-cylinder probe surpasses that of miniature wedge probes, and is comparable with that of the split-fiber thermo-anemometric probes. The PC probe is rugged, can be used in industrial flows unlike thermo-fiber probes, and its sensitivity is not adversely affected by increasing flow velocity. No involved probe angular calibration is necessary. Basically, the probe is operated as a pseudo flow follower.

The PC probe is of a simple design. It can be easily manufactured in-house, and it is relatively inexpensive. The data acquisition electronics was not discussed in the paper. It is relatively very simple. The only equipment needed is a single data acquisition channel with a high sampling rate A / D convertor and a computer with a medium size memory.

The drawback of this technology is that the probe can be reliably used only in strictly periodic flows, the test runs are longer, and the machine operation conditions must be held constant during the data acquisition period. However, unlike with TP-WP approach no labor intensive probe swapping is needed. The probe is not intended for investigations of complex transient 3D flow phenomena. It can be effectively used in 1D flows with known flow direction.

Acknowledgement

The experimental work was performed at the NASA GRC in years 2004 – 2011. The first author wishes to recognize all the help and support by former co-workers and colleagues while working on this project at NASA GRC. The support of IT ASCR for continuation of this work and enabling the authors to prepare and present this paper is also gratefully acknowledged.

References

1. J. L. Kerrebrock, A. H. Epstein, D. M. Haines and W. T. Thompkins, J. Eng. Power **96**(**4**): 394-405, (1974)
2. R. W. Ainsworth, J. J. Allen, J. J. M. Batt, J. Turbomach. **117**(**4**): 625-634, (1995)
3. P. Kupferschmied, P. Köppel, W. Gizzi, C. Roduner and G. Gyarmathy, Meas. Sci. Technol. **11**: 1036-1054, (2000)
4. C. H. Sieverding, T. Arts, R. Dénos and J.-F. Brouckaert, Experiments in Fluids **28**: 285-321, (2000)
5. J. Schlienger, A. Pfau, A. I. Kalfas and R. S. Abhari, *Measuring unsteady 3D flow with a single pressure transducer*, in Proceedings of the 16th Symposium on Measuring Techniques in Transonic and Supersonic Flow in Cascades and Turbomachines, 23-24 September, Cambridge, UK (2002)
6. J. Lepicovsky and E. P. Braunscheidel, ASME paper GT-2006-91209, (2006)
7. J. Lepicovsky, *Unsteady Pressure Measurements in Internal Aerodynamics* (in Czech), in Proceedings of the 2nd Symposium on Experimental Methods in Fluid Mechanics IT CSAV (II. Experimentálné metódy v mechanike tekutín ÚT ČSAV / in Czech), Paper 9, pp. 111-119, Poprad, (1979)
8. J. Lepicovsky, ASME Paper FEDSM-2003-45607, (2003)
9. J. Lepicovsky, ASME paper GT-2004-53954, (2004)
10. J. Lepicovsky, Report NASA/CR-2007-214815, (2007)
11. G. E Welch, *Overview of Progress in SRW/Engine research effort*, *Fundamental Aeronautics Program*, in NASA Technical Conference, Report E-663248, 13-15 March, Cleveland, USA (2012)
12. R. A. Van den Braembussche, RTO-VKI Lecture series on High Speed Pumps, Paper RTO-EN-AVT-143-13, (2006)
13. C. E. Brennen, *Hydrodynamics of Pumps*, Concepts NREC, Oxford University Press, (1994)